Proceedings of the 4th International Congress APMAS2014, April 24-27, 2014, Fethiye, Turkey

Wear Properties of TIG Surface Alloyed Steel with 50%Fe-10%W-40%B Alloy

E. Abakay[a,*], B. Kilinc[b], S. Sen[a], U. Sen[a]

[a]Sakarya University Engineering Faculity, Department of Metallurgy and Material Engineering, 54187, Serdivan Sakarya, Turkey

[b]Sakarya University, Arifiye Vocational High School, 54580, Arifiye Sakarya, Turkey

In the present study, AISI 1020 plain carbon steel was surface alloyed with preplaced 50%Fe-10%W-40%B alloying powders using a tungsten–inert gas (TIG) heat source. Microstructure, hardness, and wear resistance of the surface alloyed layer were investigated. Following the surface alloying, conventional characterization techniques such as optical microscopy (OM), scanning electron microscopy (SEM), energy dispersive X-ray spectroscopy (EDS), and X-ray diffraction analysis (XRD) were used to study the phase and microstructural examinations of the alloyed surfaces. Hardness measurements were performed across the alloyed zones, and wear properties of the alloyed surfaces were evaluated using a ball-on-disc wear test method. Hardness values of the phases formed in the alloyed layer are changing between 620±30 $HV_{0.1}$ and 2095±254 $HV_{0.1}$. The major phases formed in the surface alloyed layer were Fe_2B, FeB and FeW_2B_2. Wear test were realized against Alumina ball under the loads of 2.5 N, 5 N and 10 N at the sliding speed of 0.1 m/s for 250 m sliding distance. The friction coefficient of the 50%Fe-10%W-40%B alloyed steel surface is changing between 0.70 and 0.79 depending on applied loads. The wear rates of the surface alloyed steel ranged from 4.01×10^{-5} mm^3/m to 4.14×10^{-4} mm^3/m.

DOI: 10.12693/APhysPolA.127.957

PACS: 81.20.Vj, 81.05.Bx, 81.40.Pq, 81.65.Lp

1. Introduction

Transition metal borides have numerous useful physical and chemical characteristics that make them important materials to study. Prominent characteristics include heat resistance, great hardness, wear resistance, and high-temperature electrical resistance. Tungsten borides are resistant to thermal shock and are good thermal conductors. They are used in high-temperature applications such as crucibles and ingot molds for precision metallurgy [1, 2].

Surface alloying is a commonly employed method to improve surface properties of agricultural tools, components for mining operation, soil preparation equipments and others [3]. The surface alloying of steels, by adding the powder of a desirable composition, is a process in which the alloy powder and a thin surface layer of the substrate material are simultaneously melted and rapidly solidified to form a dense coating metallurgically bonded with the substrate. Various alloying elements such as; chromium, titanium, and tungsten may be introduced prior to or during the alloying of different steel base materials [4].

High-energy density sources have widely applied hard facing alloys such as electron beam, plasma arc and laser [5–8]. Among the welding deposition techniques, tungsten inert gas arc (TIG or GTAW) welding is a very effective and techno-economical solution for wear applications. This process has following advantages: high deposition rate, high maneuverability, large-scale availability, low cost and compatibility with a wide range of materials [9]. TIG surface alloying associated with rapid heating and cooling rate provided a unique opportunity for the non-equilibrium synthesis of materials and produced rapidly solidified fine microstructures with extended solid solution of alloying elements [10].

In the present study, AISI 1020 plain carbon steel surface was alloyed with preplaced 50%Fe-10%W-40%B alloying powders using TIG welding. The main goal of the study was to characterize the structural and dry sliding wear friction properties of the surface alloyed low carbon steels with 50%Fe-10%W-40%B.

2. Experimental

The substrate material for surface alloying treatment was prepared from AISI 1020 steel plates with the dimensions of 20 mm×60 mm×5 mm. The nominal chemical composition of the AISI 1020 steel (in wt%) was as follows: 0.17–0.38 % C, 0.18 % Si, 0.52 % Mn and Fe, the balance. Before the surface alloying treatment, these specimens were ground and cleaned with acetone to remove any oxide and grease and then dried with compressed air. Commercial ferrotungsten, ferroboron and Armco iron powders were used for the surface alloying treatment. Ferrotungsten and ferroboron were grounded by ring grinder and sieved to be 45 μm particle sizes. Surface alloying powder mixture was prepared by using a ball mill for 15 min at 120 RPM from the ground ferrous boron and tungsten powders and iron (45 μm) to be 50%Fe- 10%W-40%B. Prepared powders were placed on

*corresponding author; e-mail: eabakay@sakarya.edu.tr

the coated plate and pressed under the loads of 100 bar. Alloying powder placed on the steel plate was melted by TIG welding process. TIG welding parameters are detailed in Table I.

TABLE I
Experimental parameters of TIG surface alloying

Parameter	Value
Electrode	Type W-2 pct ThO
Diameter	2.4 mm
Angle	70 deg
Voltage	20 V
Current	110 A
Heat input	2.2 MJ/m
Protective gas	Type Ar (%99.9 Ar)
Flow	12 L/min
Welding speed	Travel speed 60 mm/min

Heat input Q = 60 x I xV/S, I: current, V: voltage, S: travel speed [11]

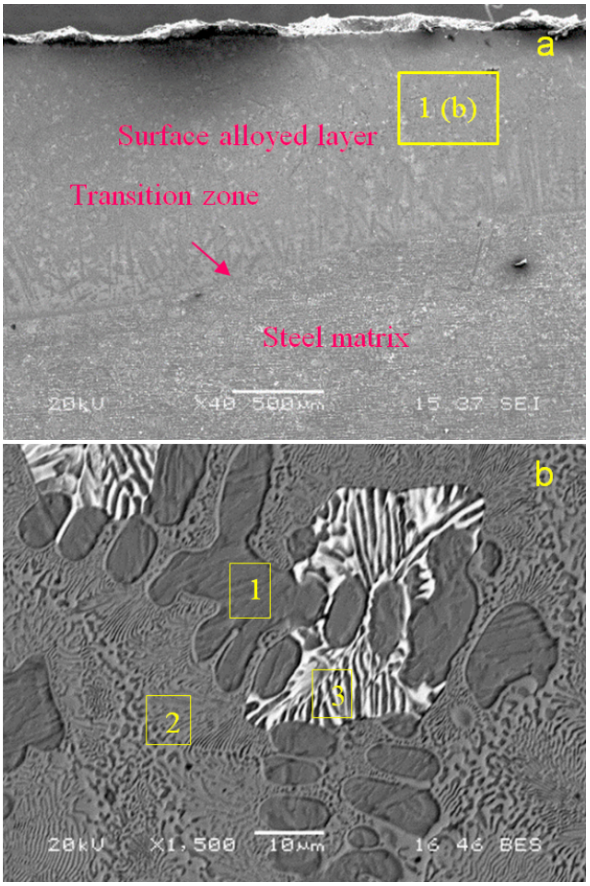

Fig. 1. SEM micrographs of surface alloyed AISI 1020 steel.

The phase analysis was realized using a Rigaku XRD/D/MAX/2200/PC X-ray diffractometer with Cu K_α to analyze the constituent phases in the surface alloyed layer. Metallographic examinations on the metallographically prepared and etched samples with 3% nital for 10 s were realized from the cross-section of the surface alloyed layer using by Nikon Epiphot 200 optical microscopy (OM) and JEOL JSM - 6060 scanning electron microscopy (SEM). The hardness of the phases formed in the alloyed layer and transition zone and matrix were measured from the cross-section by Future-Tech FM 700 micro-hardness tester.

Wear and friction tests of the surface alloyed steels were evaluated using a ball-on-disc tribometer in the atmospheric condition (62% relative humidity). The samples with 20 mm×20 mm×5 mm were cut from as received TIG melted 50%Fe-10%W-40%B alloy on the steel substrates and were ground by 1200 grit silicon carbide papers for obtain a smooth surface. The sliding speed was 0.1 m/s; the applied loads were 2.5 N, 5 N and 10 N and the sliding distance was 250 m. Mean Hertzian contact pressures [12] calculated for alumina ball under the loads of 2.5 N, 5 N and 10 N are 390 N/mm^2, 490 N/mm^2 and 620 N/mm^2, respectively. The frictional force, monitored by a load cell attached to the ball holder, was recorded continuously. Wear rate was measured primarily by volumetric (volume loss) means. To evaluate wear resistance, the wear volume was calculated from the worn cross-sectional area of the surface alloyed plate which was measured by KMA P6 optical profilometer.

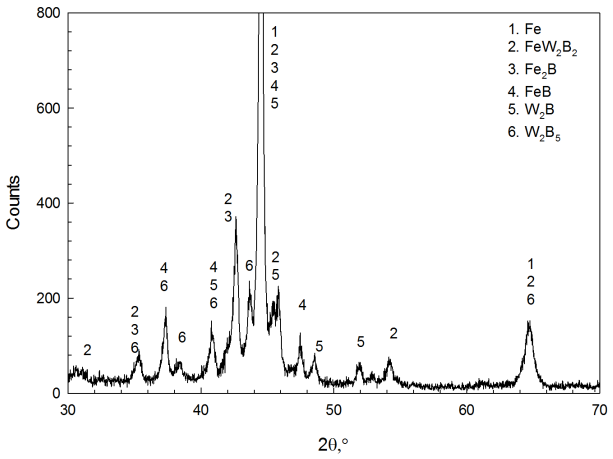

Fig. 2. X-ray spectrum of surface alloyed layer on AISI 1020 steel.

3. Results and discussion

Surface alloying process was applied on AISI 1020 steel substrates. The treatment was realized by ferrotungsten, ferroboron and Armco iron as filler alloys as to be 50%Fe-10%W-40%B. The composition of the filler alloy mixtures of ferrotungsten, ferroboron and iron powders were calculated and used for the production of Fe_2B, FeB and FeW_2B_2 major phases in the final produced alloy according to Fe-W-B phase diagram [13]. As known, the borides of iron and FeW_2B_2 phases have very high hardness, wear resistance and corrosion resistance [13–15]. In the process, prepared powder mixture was melted on the steel samples and simultaneously rapidly solidified to form a dense coating bonded on the base metal.

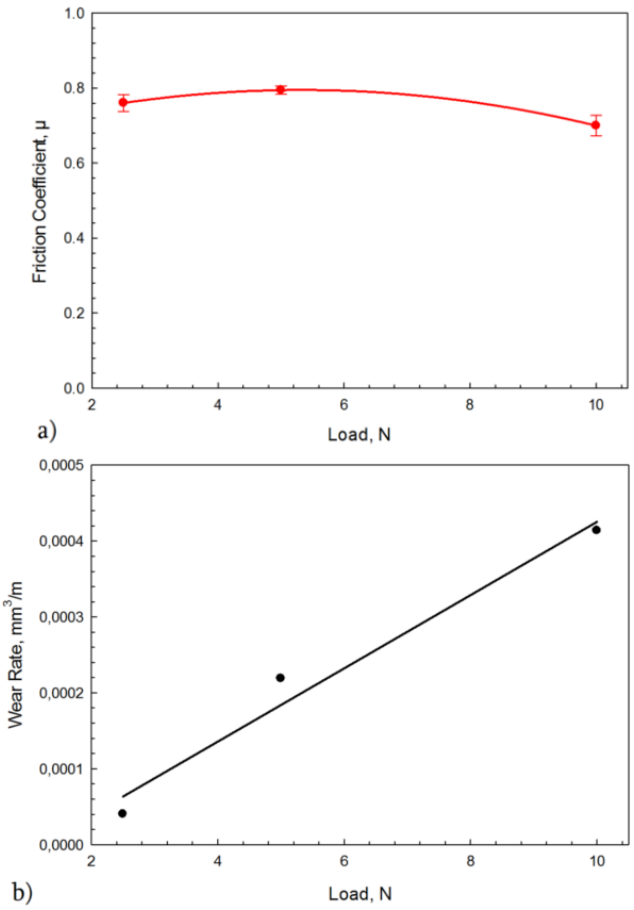

Fig. 3. (a) Friction coefficient and (b) wear rate variation of surface alloyed.

Figure 1a shows the lateral section of the surface alloyed steel. The figure shows that surface alloyed steel samples include three distinct regions which are: i) surface alloyed layer which includes Fe, B and W, ii) transition zone and iii) steel matrix. According to Fig. 1a, surface alloyed layer gave a smooth rippled surface topography and was found to be free from gas porosity and cracks in general. Figure 1b show the surface alloyed layer microstructure. As shown from the figure that solidificated microstructure includes primary dendrites of the Fe-W solid solution (marked as 1 on the micrograph), eutectic microstructures of $Fe+Fe_2B$ (marked as 2 on the micrograph) and FeW_2B_2+Fe eutectic (marked as 3 on the micrograph) which were investigated by EDS analysis.

Figure 2 shows the XRD analysis of surface alloyed AISI 1020 steel with 50%Fe- 10%W-40%B alloy. The analysis showed that the layer includes Fe_2B, FeB and FeW_2B_2 phases as major and W_2B and W_2B_5 phases as trace [13].

In the alloying treatments, solidification of the melted zones is too speed and it is possible that the formation of some deal phases of the used elements can be realized because of sufficient time for the production of stable phases took place in the phase diagram of the Fe-W-B [13].

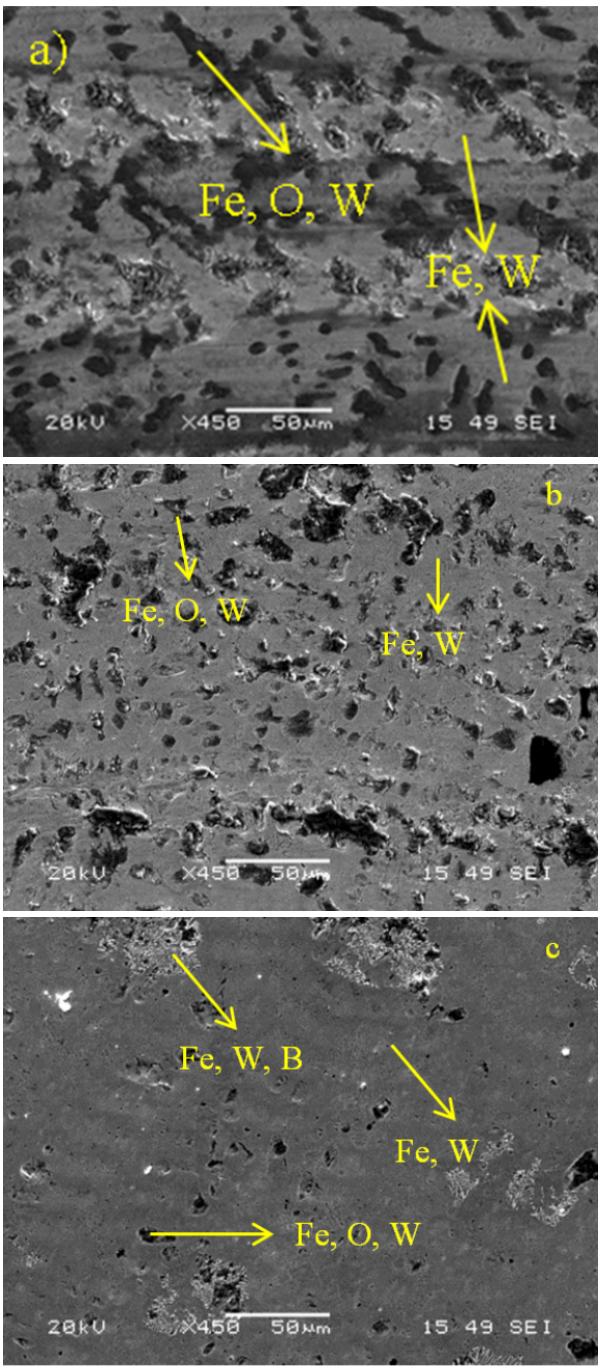

Fig. 4. SEM micrographs of the worn surfaces of the surface alloyed AISI 1020 steel with 50%FE-10%W-40%B, alloys for (A) 2.5N, (B) 5N and (C) 10N load.

Figure 3a shows the variation of friction coefficients as a function of applied load against alumina ball at the sliding speed of 0.1 m/s for 250 m sliding distance. It seems from this figure that increases in applied load do not caused to change of friction coefficient, effectively.

Figure 3b presents the wear rate of the surface alloyed AISI 1020 steel against alumina ball. As shown from the figure that increase in applied load caused to increase of

wear rate for all loads. Archard's equation shows that increasing load reasoned the increase of wear rate [16]. The load is effective parameters in the wear test which is caused to increase of wear rate. Increase in applied load 100% caused to increase in wear rate of 446% increase in applied load 300% caused to increase of 932%.

AISI 1020 steel with increased loads, respectively.

Figures 4b and 4c show the wear tracks of surface alloyed AISI 1020 steel under the loads of 2.5 N, 5 N and 10 N, respectively. SEM images and EDS analysis showed that oxidative wear products realized on the wear track and abrasive micro abrasive wear scratches. Wear of the surface alloyed layer is largely oxidative in nature under 2.5 N and 5 N. Increasing of applied load, changed wear mechanism from oxidative to abrasive for 10 N loads.

4. Conclusions

1. Surface alloying process was applied on AISI 1020 steel substrates by TIG welding.
2. Surface alloyed layers of the steel consist of Fe_2B, FeB and FeW_2B_2 phases.
3. The surface alloyed steel samples include three distinct regions which are surface alloyed layer which includes Fe, B and W, transition zone and steel matrix.
4. The surface alloyed layer includes primary dendrites of the Fe-W solid solution, eutectic microstructures of Fe+Fe_2B and FeW_2B_2+Fe eutectic.
5. XRD analysis of surface alloyed AISI 1020 steel showed that the layer includes Fe_2B, FeB and FeW_2B_2 phases as major and W_2B and W_2B_5 phases as trace.
6. The friction coefficient is close for 2.5 N and 5 N applied loads (0.77–0.79) and with increasing of the load from 5 N to 10 N, the friction coefficient decreased from 0.79 to 0.70.
7. Increase in applied load caused to increase of wear rate.
8. Wear mechanism of the surface alloyed AISI 1020 steel is for 2.5 N and 5 N loads oxidative and for 10 N oxidative and abrasive.

References

[1] S. Stadler, R.P. Winarski, J.M. MacLaren, D.L. Ederer, J. vanEk, A. Moewes, M.M. Grush, T.A. Callcott, R.C.C. Perera, *Journal of Electron Spectroscopy and Related Phenomena* **110**, 75 (2000).

[2] M. Usta, I. Ozbek, M. Ipek, C. Bindal, A.H. Ucisik, *Surface and Coatings Technology* **194**, 330 (2005).

[3] M.F. Buchely, J.C. Gutierrez, L.M. León, A. Toro, *Wear* **259**, 52 (2005).

[4] S.M.H. Hojjatzadeh, A. Halvaee, M. Heydarzadeh Sohi, *Journal of Materials Processing Technology* **212**, 2496 (2012).

[5] V. Balasubramanian, R. Varahamoorthy, C.S. Ramachandran, C. Muralidharan, *The International Journal of Advanced Manufacturing Technology* **40**, 887 (2009).

[6] J.C. Oh, S. Lee, *Surface and Coatings Technology* **179**, 340 (2004).

[7] A. d'Oliveira, R.S.C. Paredes and R.L.C. Santos, *Journal of Materials Processing* **171**, 167 (2006).

[8] P.W. Leech, *Materials and Design* **54**, 539 (2013).

[9] R.A. Jeshvaghani, M. Jaberzadeh, H. Zohdi, M. Shamanian, *Materials and Design* **54**, 491 (2013).

[10] D. Deng, Y. Zhou, T. Bi, X. Liu, *Materials and Design* **52**, 720 (2013).

[11] S. Buytoz, *Surface and Coatings Technology* **200**, 3734 (2006).

[12] B. Stingl, M. Ciavarella, N. Hoffmann, *International Journal of Mechanical Sciences* **72**, 55 (2013).

[13] V. Raghavan, *Journal of Phase Equilibria* **24**, 457 (2003).

[14] O. Ozdemir, M. Usta, C. Bindal and A.H. Ucisik, *Vacuum* **80**, 1391 (2006).

[15] I. Campos, M. Palomar, A. Amador, R. Ganem and J. Martinez, *Surface and Coatings Technology* **201**, 2438 (2006).